11 Diode-Laser Sensors for In-Situ Gas Analysis

Peter Werle

11.1 Absorption Spectroscopy

Optical sensors based on semiconductor lasers are at the threshold of routine applications in gas analysis and increasingly these sensors are used for industrial and environmental monitoring applications whenever sensitive, selective and fast in-situ analysis in the near- and mid-infrared spectral region is required. With the increasing complexity of processes, online gas analysis is becoming an issue in automated control of various industrial applications such as combustion and plasma diagnostics, investigations of engines and automobile exhaust measurements. Other challenges are online analysis of high purity process gases, medical diagnostics and monitoring of agricultural and industrial emissions (VDI 2002). The need to meet increasingly stringent environmental and legislative requirements has led to the development of analyzers to measure concentrations of a variety of gases based on near- and mid-infrared absorption spectroscopy.

Absorption spectrometers generally contain a radiation source and an appropriate detector together with the species under investigation in an absorption cell for concentration measurements based on Beer´s law. As a prerequisite to obtain the required selectivity a dispersive element has to be inserted in to the optical path. Modern gas analyzers use semiconductor lasers, where the selective element is the radiation source itself. Various techniques and designs have been developed to meet specific requirements of different measurement challenges and for high sensitivity in-situ applications several techniques are available. In photo-acoustic spectroscopy (see chap. 16) intensity modulated light is absorbed by a target gas at a specific wavelength. The absorbed photon energy is transformed into translation energy by collisions, resulting in a modulation of gas temperature and pressure respectively. Using a sensitive microphone to measure this signal, very low concentrations can be detected. Photo-acoustic trace detectors have shown their value in the fields of medical sciences (e.g. breath tests, see chap. 12) and environmental studies. Cavity ring down (see chap. 7 and 14) spectroscopy is an other sensitive absorption technique in which the rate of absorption rather than the magnitude of the absorption of a light pulse confined in an optical cavity is measured.

Tunable diode-laser absorption spectroscopy (TDLAS) is increasingly used as an attractive technique for analytical instrumentation. In such instruments a single narrow laser line is tuned by injection current changes over an isolated absorption line from ν_1 to ν_2 of the species under investigation (Fig. 11.1a). To achieve the highest selectivity, analysis is made at low pressure, where absorption lines are not substantially pressure broadened. This type of measurements has developed into a very sensitive and general technique for monitoring atmospheric trace species (Schiff et al. 1994). The main requirement is that the molecule should have an infrared line-spectrum which is resolvable at the Doppler limit, which in practice includes most molecules with up to five atoms (as for example CO, CO_2, NO, N_2O, NO_2, HNO_3, NH_3, CH_4, CH_2O, H_2O, H_2O_2) together with some larger molecules. Because TDLAS operates at reduced pressure it is not restricted in wavelength to the atmospheric windows at 3.4-5 µm and 8-13 µm. Direct absorption measurements have to resolve small changes ΔI in a large signal offset I_0. Therefore, most applications of TDLs in atmospheric research required long-path absorption cells to provide high sensitivity local measurements (Brassington 1995).

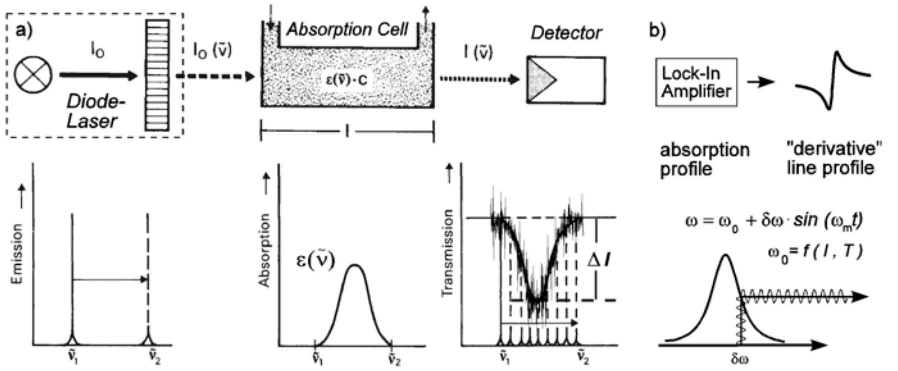

Fig. 11.1a. Diode-laser absorption spectroscopy **b.** wavelength modulation spectroscopy

Signal averaging increases the signal-to-noise ratio (SNR) and for signal levels $\Delta I/I_0$ below 10^{-3} additional noise suppression can be achieved by the application of modulation techniques. In modulation spectroscopy, the laser injection current is modulated at ω_m while the laser wavelength is tuned repeatedly over the selected absorption line to accumulate the signal from the lock-in amplifier with a digital signal averager (Fig. 11.1b). This produces a derivative line profile with an amplitude proportional to the species concentration. Scanning over the line gives increased confidence in the measurement, because the characteristic spectrum of the measured species is clearly seen and unwanted spectral features due to interfering species or étalon fringes can easily be identified. The benefits of modulation spectroscopy are twofold : Firstly, offsets are eliminated (zero baseline technique) as it produces a derivative signal, directly proportional to the species concentration and, secondly, it allows narrowband detection of the signal at a frequency at which the laser noise is reduced.

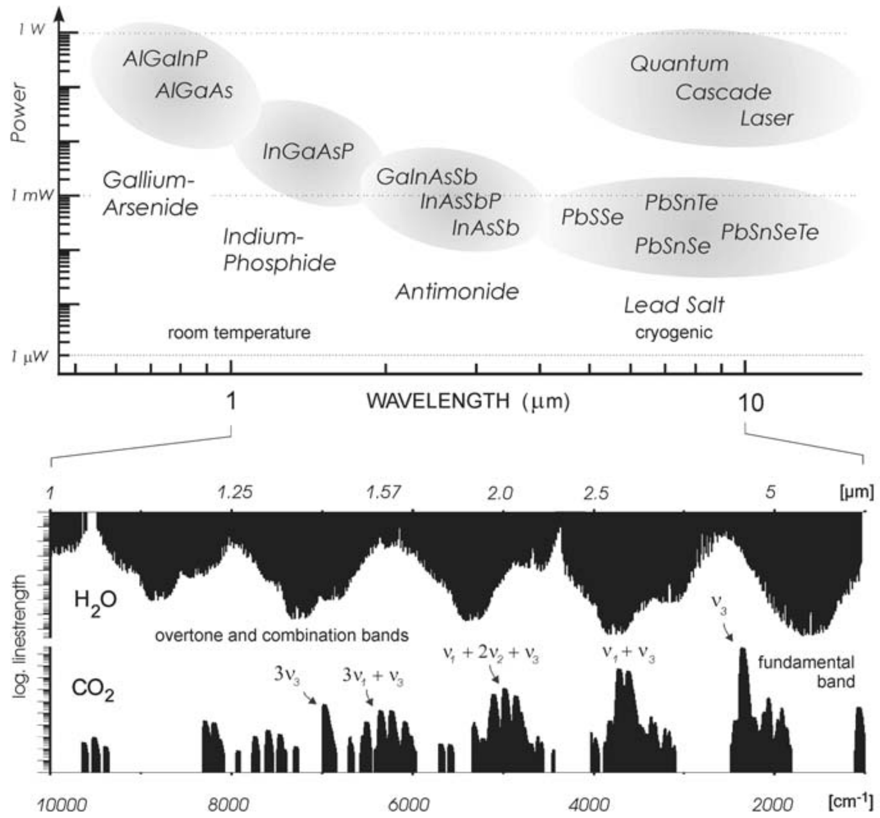

Fig. 11.2. Typical available diode-laser continuous wave output power versus spectral coverage of the visible to infrared region by different semiconductor material systems together with an example of absorption cross sections for CO_2 and interfering water vapor (Rothman et al. 1992)

Different molecules show absorption of light at different wavelengths based on their fingerprint-like absorption spectrum (Fig. 11.2). In the spectral range from the visible to the infrared combination and overtone bands as well as the fundamental bands can be covered by diode-lasers based on Gallium-Arsenide, Indium-Phosphide, Antimonides and Lead-salts (Werle et al. 2002) and the recently developed quantum cascade lasers (QCL) (Faist et al 1994, Beck et al. 2002). While in the past only mid-infrared diode-lasers operated at cryogenic temperatures covered the fundamental absorption bands required for high sensitive gas analysis, near-infrared room temperature diode lasers gave access only to the significantly weaker overtone and combination bands. Therefore, the selection of the operating regime for a gas analyzer is always a trade off between the required sensitivity, system complexity and operational cost. While predicted sensitivities are based on known line strengths and system performance, it is in the nature of field measurements that optimum performance is not always achieved due to instrumental drifts, interferometric effects and turbulent refractive index fluctuations. To cope with these problems, for example approaches based upon signal-processing and double modulation techniques (Werle and Lechner 1999) have been successfully applied.

To illustrate the performance and operation of near- and mid-infrared spectrometers based on tunable diode-lasers, in the next sections selected applications of spectrometers applying lead-salt diode-lasers for NO_2 and CH_4 sensing, antimonide lasers for CH_4 and HCHO sensing in the 3-4 µm range and a near-infrared gas sensor for CO_2 based on a room temperature 2 µm Indium-Phosphide laser will be presented. Finally, the impact of the mid-infrared quantum cascade lasers on spectrometer performance that has been obtained so far will be discussed.

11.2 Mid-Infrared Diode-Laser Spectrometers

Historically, the first measurements with diode-lasers have been made with mid-infrared lead-salt devices. They are based on IV-VI semiconductor materials and operate in the 3 to 30 µm spectral region (Tacke 1995). Lead-salt lasers cover the IR fundamental bands with strong absorption for the most atmospheric trace gases and are used almost exclusively environmental research (Fried et al. 1997, Fischer et al. 2000, Kormann et al. 2001) and for spectroscopic applications. In trace gas monitoring applications, lead-salt laser instruments have routinely achieved parts-per-billion (1 ppbv = 10^{-9} volume mixing ratio) detection levels of a number of important molecular species. For unattended industrial routine applications the use of lead-salt diode lasers is limited by the need of cryogenic cooling (LN_2 or Stirling coolers, typical 78-120 K), the occurrence of multimode emission and power levels, which are typically several hundred microwatts. Compared to GaAs lasers, lead-salt diode-lasers are at a relatively early stage of their development due to a much smaller market. In order to improve TDLAS detection speed and detection limits high frequency modulation (FM) techniques have been introduced. These techniques determine the absorption or dispersion of a narrow spectral feature by detecting the heterodyne beat signal that appears when the optical spectrum of the probe wave is distorted by the spectral feature of interest. Advances in laser-optical gas analyzers based on these techniques have been reviewed (Werle 1998) and therefore only the essentials will be summarized here. The major difference to conventional modulation spectroscopy is the application of radio frequency modulation (rf) instead of conventionally used kHz frequencies. This allows faster scanning and signal detection at MHz to GHz frequencies, where laser excess noise does not dominate detection and therefore, in principle, a detection limit close to the quantum limit can be obtained (Werle et al. 1989). In a FM spectrometer a rf-current of typically about 100 MHz is used to modulate a DC current with a superimposed ramp via a bias-T to decouple the different current sources. The modulated current, $i_L(t)$, generates a frequency modulated electromagnetic field, $E_1(t)$, which interacts resonantly with the rotational-vibrational absorption of the molecules in the sample cell. The number of photons emitted from the laser depends upon the number of electrons in the conduction band and, therefore, from the current through the pn-junction of the diode laser. The higher the current, the higher the number of photons available and the amplitude of the electromagnetic field depends on photon density, i.e. changes in the laser current will lead to an amplitude modulation of the laser. The index of refraction in the pn-junction of the laser depends on the carrier density. Therefore, there is a coupling between amplitude and frequency modulation for the electric field. The phase modulated electrical field, $E_1(t)$, with residual amplitude (AM) modulation is

$$E_1(t) = E_0(t)\cdot [1+M \sin(\omega\, t+\psi)] \;\cdot \exp\{\, i\, (\Omega\, t + \beta \sin(\omega\, t))\}, \tag{11.1}$$

where $\omega \equiv$ modulation frequency, $\Omega \equiv$ laser carrier frequency, $\beta \equiv$ FM-index, $M \equiv$ AM-index and $\Psi \equiv$FM-AM-phaseshift. For low modulation indices we obtain in the frequency domain an upper and a lower sideband, which are displaced $\pm\omega$ from the laser carrier Ω. The principle setup of a FM-TDLAS system is shown in Fig. 11.3a. A fraction of the original laser beam is required for active line locking using the reference channel, while about 90% of the laser intensity is used for the sample gas detection in a multipass absorption cell. The electrical field, $E_2(t)$, after interaction with the sample can be described by

$$E_2(t) = E_1(t)\, exp\{-\, \delta(\omega) - i\phi(\omega)\} \tag{11.2}$$

where $\delta(\omega)$ is the absorption and $\phi(\omega)$ is the dispersion of the sample gas. The electrical field after the probe induces a detector current, $i_{\mathrm{rf}}\,(t)$, in a photovoltaic Mercury Cadmium Telluride (MCT) detector.

$$i_{\mathrm{rf}}\,(t) = /\, E_2(t\, /^2 \tag{11.3}$$

The amplified and filtered current is fed into the rf-input of a double balanced mixer for phase sensitive detection at the modulation frequency. For a selected phase shift between the local rf-oscillator i_{LO} and the detector signal i_{rf} we record at the intermediate frequency IF mixer output port the lowpass (τ) filtered product

$$i_{\mathrm{IF}}\,(t) = \langle\; i_{\mathrm{LO}}\,(t) \cdot i_{\mathrm{rf}}\,(t) \;\rangle_\tau \tag{11.4}$$

After this phase sensitive detection at the modulation frequency, the demodulated signal, $i_{\mathrm{IF}}(t)$, is proportional to the concentration of the trace gas in the absorption cell and by adjusting the detection phase either the absorption or the dispersion signal can be selected (Werle 1998). The reference beam passes through a reference cell, which provides at high signal-to-noise ratio a signal from the spectral feature under investigation. This channel is used for line-locking and online drift correction. A line locking procedure monitors the deviation of the signal position from a given set-point and compensates for drifts. The sample and the reference signals are then digitized and further processed by digital filters, line locking algorithms, calibration procedures and an intensity normalization to cope with laser power fluctuations (Werle et al. 1994). The corrected signals are then further stored in a computer for digital signal processing and referenced to a previously recorded calibration spectrum to provide final concentrations in different units (ppbv, molec/cm^3, µg/cm^3) together with the calculated measurement precision.

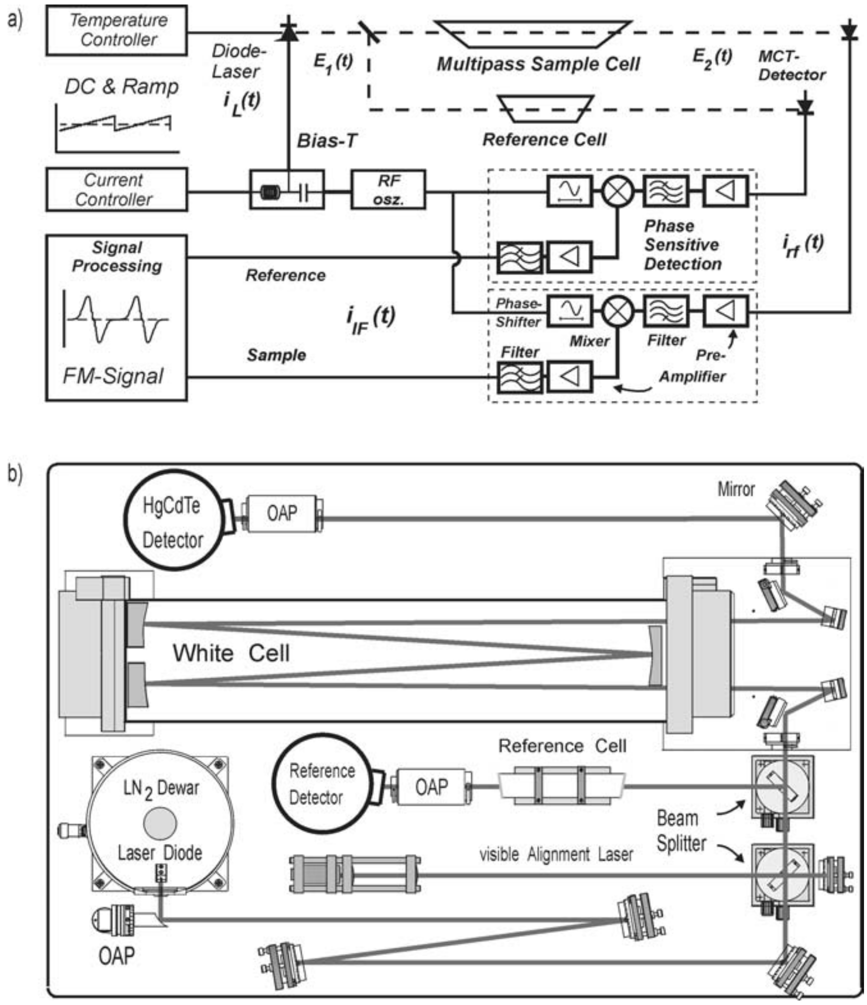

Fig. 11.3a. FM-detection scheme **b.** Mid-infrared lead-salt diode-laser spectrometer

The mid infrared TDLAS system shown in Fig. 11.3b is based on lead-salt lasers and has been used for spectroscopic in-situ detection of NO_2. For the experiments a lead-salt diode-laser was mounted in a liquid-nitrogen (LN_2) cooled dewar, which has been used for a spectral characterization in a laser test setup prior to the spectroscopic measurements. To accommodate for a possible deviation angle between the cone of laser emission and the laser mount axis, the LN_2 - dewar is mounted on a xyz-stage alignable within ± 30°. The beam from the TDL is first collimated by an off-axis parabola (OAP) and then directed by a sequence of mirrors through the sample cell and onto a LN_2-cooled HgCdTe photovoltaic detector.

A visible alignment laser beam can be combined via a pellicle beam splitter with the invisible infrared beam to assist during the system alignment phase. For typical line-strengths an ambient concentration of 1 ppbv produces an absorption of only 1 part in 10^7 over a 10 cm path-length. Conventional absorption spectroscopy would not be able to measure such small absorption. TDLAS overcomes this problem by using a multi-pass cell with folded optical paths of 100 m or even more (White 1976, Herriott and Schulte 1965). The White cell used in this system has a base length 62.5 cm and an adjustable path length, L, of up to 100 m. For optimum SNR, the absorption path length is adjusted to 27.5 m. The system operates at a gas flow of 10 l/min and the pressure inside the cell is actively regulated using a MKS Baratron to maintain a pressure of 26.7 hPa. The optical setup is mounted on a 100 x 60 cm optical breadboard and is enclosed in a box flushed with dry nitrogen to improve the thermal stability. The frequency of the laser was tuned over the selected NO_2 absorption. For NO_2 measurements an absorption line at 1600.413 cm^{-1} was chosen since its background was free of disturbance from the pressure broadened H_2O lines nearby. The NO_2 line consists of two unresolved lines of equal line strength of $1.17 \cdot 10^{-19}$ cm/molecule.

Trace gas measurements near to the detection limit are usually performed by measuring the ambient air spectrum and the spectrum of zero air, i.e. air devoid of the target substance, which is referred to as the background spectrum. The background spectrum still contains the disturbing spectral signatures from interfering fringes and therefore can be subtracted from an ambient spectrum to obtain a clean spectrum. Another prerequisite for quantitative measurements is a calibration spectrum, which can for example be obtained by measuring gas from a commercial certified gas cylinder after dilution to the required concentration level. For calibration purposes higher concentrations are usually used with corresponding signals that are much larger than the fringes in the spectrum. Provided that the laser frequency is kept constant by line locking, the acquisition of the calibration spectrum can then be omitted from the measurement sequence. This is advantageous since a substantial part of the time is needed to exchange the gas in the White cell after switching from ambient air to zero air for background recording.

The instrument performance in terms of the detection limit and detectable optical density has been determined from NO_2 measurements in ambient air. A calibration, background and ambient spectrum as well as the background corrected spectrum is shown in Fig. 11.4a, where 256 spectra have been averaged within 740 ms. The electronics bandwidth of 1.5 kHz leads to an effective bandwidth of 5.86 Hz. The mixing ratio of NO_2 was calculated by least square fitting to the calibration spectrum taken at 12 ppbv (1ppbv = 10^{-9} volume mixing ratio). From a least squares fit a mixing ratio of 1.17 ppbv with a 1 σ precision of 31.5 pptv has been obtained. For quality assurance additional quantitative information on system stability and the maximum signal averaging time has been derived from an Allan variance analysis, which has been discussed in detail together with the aspects of background stability by Werle et al. 1993. An Allan plot has been generated from a continuous measurement of zero air spiked with 12 ppbv of NO_2 from a calibration source for a period of 600 s with a time resolution of 1.5 s. As the linearly decreasing part of the Allan variance is dominated from white noise, it is in this part equivalent to the statistical variance and, consequently, the square root of the Allan variance gives a prediction of the detection limit. From the recorded time series data in Fig. 11.4b we obtain for an integration time of 25 s a detection limit of 10 pptv from the Allan variance, corresponding to a detectable change in optical density of $5 \cdot 10^{-7}$. At longer integration times the Allan variance, and with it the instrument detection limit, will start to deteriorate as a consequence of instrumental drifts. In practical terms this means that the complete measurement sequence consisting of the acquisition of the ambient, background and calibration gas spectra has to be completed within 60 s.

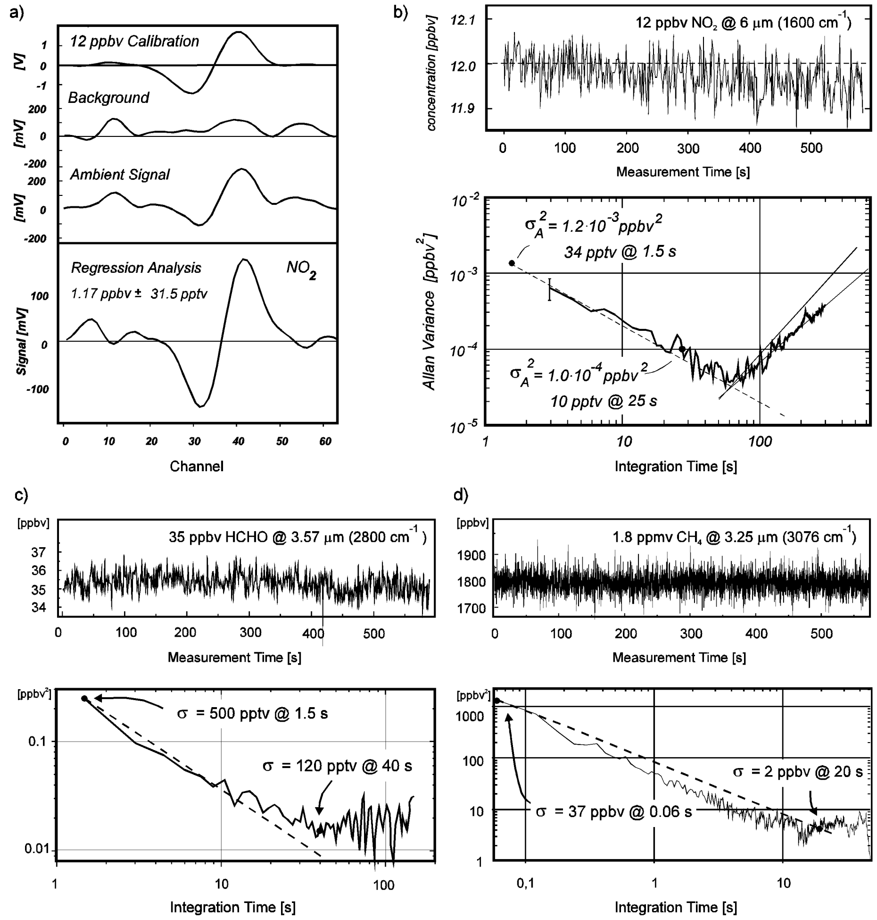

Fig. 11.4a. calibration, background and ambient spectra for NO_2 and **b-d.** time series data and corresponding Allan Plot (Werle et al. 1993) for NO_2, H_2CO, CH_4

The number of manufacturers for lead-salt diode-lasers is limited world-wide to one or two, which changes slightly from time to time. Therefore, alternatives in the infrared spectral region are desperately asked for. For wavelengths below 4 µm down to 1.8 µm Antimonide lasers, based on III-V compounds such as AlGaAsSb, InGaAsSb, and InAsSbP, can be used (Nicolas et al. 1998). Room temperature lasing from 2 to 2.4 µm has been reported from simple double heterostructure antimonide diode-lasers. As wavelength increases up to 3.7 µm, the maximum operating temperature decreases as a result of increasing optical and electrical losses. Laser devices used in the experiments described here are based on InAsSb/ InAsSbP double heterostructure devices and were grown by liquid phase epitaxy on InAs substrate at the Ioffe Physico Technical Institute in St. Petersburg, Russia and cover the spectral range from 3-4 µm at LN_2 temperatures. Such devices are well suited for the detection of HCHO at 3.6 µm and CH_4 at 3.26 µm (Werle and Popov 1999). For gas sensing applications lasers have been selected for formaldehyde emitting at 3.57 µm (2800.2 cm^{-1}) and for methane operating at 3.25 µm (3076.5 cm^{-1}). For the formaldehyde measurements the previously described NO_2 instrument with the 6 l White cell now at L=30 m total pathlength and a pressure of 30 hPa has been used. From experiments we determined a detection limit for HCHO of 120 pptv with 40 s integration time (Fig. 11.4c) or in terms of minimal detectable optical density $(\alpha L)_{min} = 10^{-6}$ at $\Delta f = 1$ Hz. The methane measurements aimed at a higher time resolution for flux measurements and the White cell was replaced by a 5 l Herriott cell with a total pathlength of 100 m. For CH_4 a precision of 37 ppb has been obtained with 0.06 s integration time corresponding to $(\alpha L)_{min} = 2.7 \cdot 10^{-4}$ at $\Delta f = 1$ Hz (Fig. 11.4d). While the results for formaldehyde were quite satisfying, the performance of the methane measurements was worse due to the fact that the spectral response of the HgCdTe detectors is degrading near 3 µm. Furthermore the relative low power of 200 µW and the 100 m optical pathlength with the corresponding strong power attenuation due to multiple reflection (Werle and Slemr 1991) led to a low power level at the detector. With an optimized system with respect to optical power transmission and an antimonide laser that emits at higher injection currents, providing higher power, the potential of the increased line strength in the ν_3 band of CH_4 according to the Hitran database (Rothman et al. 1992) should be feasible. Antimonide lasers might offer operational benefits compared to lead-salt lasers, while still maintaining high sensitivity by probing fundamental ro-vibrational absorption transitions.

Modern atmospheric research on gas exchange between the biosphere and the atmosphere requires sensitive, reliable and fast-response chemical sensors. Therefore, techniques for fast and simultaneously sensitive trace gas measurements based on tunable diode-laser absorption spectroscopy have been successful applied to micrometeorological trace gas flux measurement techniques as the eddy covariance technique (Zahniser et al. 1995, Kormann et al. 2001). The availability of such sensors allows for example a validation of closed chamber measurements and also can provide information about CH_4 emissions on a larger scale, which is the basis for any up-scaling effort from a regional to a global scale.

The eddy correlation technique directly determines the flux of an atmospheric constituent through a plane that is parallel to the surface. Ideally, the meteorological conditions controlling the state of the turbulence should not vary over the course of the measurements and the surface viewed by the sensors should be horizontally uniform, both in its physical and chemical-biological aspects. Because the eddy correlation method may be considered as defining the instantaneous upward or downward transport of the constituent and then averaging contributions to give the net flux, it must take into account the frequency range of the turbulence for vertically transporting the constituents in the atmosphere. The technique requires simultaneous fast and accurate measurements of the vertical wind velocity and the concentration of the trace species in question.

The key element of such a field instrument is the diode-laser. When starting to select a laser, the first task is to select from mode maps a combination of base temperature and drive current at which the laser produces a strong, preferably single mode emission, tuned to the absorption line being monitored. Due to the limited sensitivity obtained with the antimonide laser described before, a 7.8 µm (ν_4-band) lead-salt diode-laser was the optimum choice for CH_4 flux measurements. The optomechanical components of the spectrometer are mounted on an 50 x 90 cm optical breadboard (Fig. 11.5a). The lead-salt diode-laser is mounted on a cold-head within a LN_2-dewar. For injection currents between 400 and 600 mA at temperatures ranging from 85 to 95 K single mode operation (Fig 11.5b) with an average power level of 200 µW was ensured and isolated CH_4 absorption lines could be reproducibly selected for the measurements even after repetitive thermal cycling, which was an important criterion for the planned field measurements.

The experimental setup of the eddy correlation system has been described in detail by Werle and Kormann 2001 and is similar to the one shown in Fig. 11.3. The White cell has been replaced by a Herriott cell with a very small internal volume of 0.3 l designed for applications requiring fast gas flow and exchange to allow high time resolution. A rotary vacuum pump provides the gas flow of about 18 slm through the Herriott cell at a pressure of about 50 hPa. A dust filter is at the inlet of the measurement head to protect the gas system and the mirrors of the Herriott cell from pollution. A calibration system allowed programmed sequences of measurements of background signals, calibration gas and ambient air. The calibration system is based on a dynamic gas dilution system, where calibration gas from steel cylinders is diluted with N_2 down to ambient concentration levels. With this spectrometer ambient methane concentrations around 2 ppmv can be detected with a precision better than 1 % at a 10 Hz repetition rate and a typical 30 min data set contains 18000 individual concentration values (Fig. 11.5c). Each concentration value has been obtained by averaging individual spectra followed by a background correction as described previously. The “noisy” structure in the high resolution time series data reflects the turbulent nature of transport in the atmosphere and has frequency contributions from 0.01 Hz up to 10 Hz. For each concentration measurement the corresponding vertical wind speed has been measured.

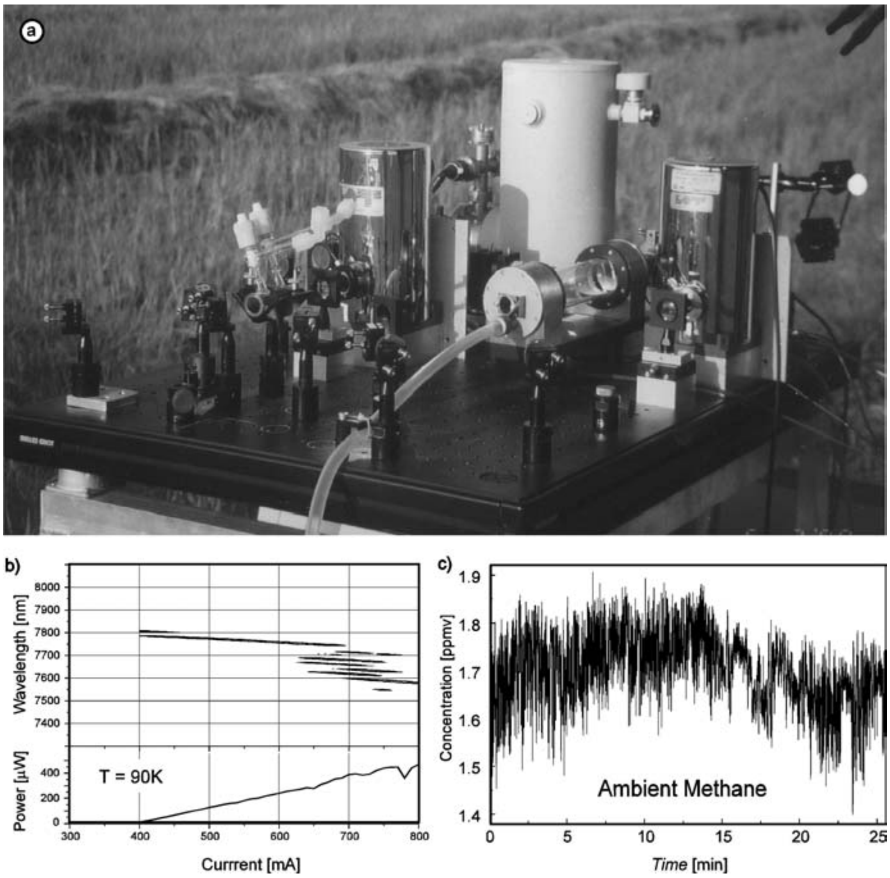

Fig. 11.5a. fast chemical "field" spectrometer with laser and detector dewars and small volume Herriott cell for eddy correlation trace gas flux measurements during a measurement campaign in Italian rice paddy fields (Werle and Kormann 2001). **b.** mode map of a lead-salt diode-laser **c** time series data of ambient methane concentrations with 10 Hz time resolution

The continuous gas flow of the ambient air into the measurement cell of the spectrometer introduces an uncertainty into the simultaneity of time series wind and concentration data. Therefore, a correlation analysis was used to find the time lag and the fluxes. The first step in the eddy correlation process is to calculate the perturbation values of the data points. For the measured time series of concentration values we subtract the mean from each data point to yield a time series of perturbations c′. We can similar find a time series of vertical wind velocity perturbations w′. Multiplying the respective values together yields a time series w′c′. The average of this series <w′c′> gives the turbulent vertical flux. An advantage of this method is that it is direct and simple, and fluxes can be calculated at whatever height or location the original time series was measured.

In the frame of an interdisciplinary research project eddy correlation measurements of methane emissions from rice paddy fields have been performed during a field campaign to allow a comparison with data from a set of on-site monitoring systems based on the closed chamber technique. A typical gas collection chamber covers a surface of about 0.4 m^2 and is fitted with a removable plexiglass. The methane emission rate is calculated from a temporal increase of CH_4 inside the box during a 30 min closure time using a gas chromatograph. Spatial variability is a great problem in using chambers to measure fluxes from a field or ecosystem. In addition, chambers disturb the natural air turbulence, decouple the rice plant from the ambient turbulent atmosphere and alter the temperature, solar radiation and gas concentration in the measurement environment. Therefore, the extrapolation of methane emissions, based on flux rates obtained by use of small closed chamber measurements, to field, landscape and regional levels is not so well established.

The measurements based upon the ´state-of-the-art´ closed chamber technique report about 60-90% higher methane emissions than the simultaneous eddy correlation measurements (Werle and Kormann 2001). The lower fluxes measured by the micrometeorological eddy correlation system have been confirmed in an on-site comparison with two other independent diode-laser based eddy correlation systems. All participating instruments (laser spectrometers and gas chromatographs) were calibrated routinely and simultaneous measurements of ambient methane *concentrations* reported the same values and it is important to point out that the differences occurred only for the *fluxes* calculated from the different techniques. As a first attempt to try to explain this difference, we may recall that closed chambers usually have a fan mounted inside the chamber and during closure, the fan causes rapid mixing of air within the chamber. Thus a strong artificial turbulence is introduced in the chamber, which does not allow natural gradients inside the box. The chamber data may suffer from this experimentally introduced effect, which might have influenced methane flux measurements by closed chambers in rice paddy fields so far. While the amount of distortion or turbulence is constant inside the chamber and decoupled from the atmospheric conditions, this is not the case for the almost unaffected in-situ eddy correlation measurements in the free atmosphere. Other findings indicate that for higher wind speed the difference between eddy correlation data and closed chamber measurements becomes smaller, but unfortunately, in the rice growing regions wind speed tends to be low and the problem remains. Whatever the process is, that causes more flux in the closed chamber with fans on, so far the consensus is that it only accounts for a fraction of the difference between chambers and micrometeorological measurements. The discrepancy between micrometeorological measurements and the closed chamber technique has not been resolved completely yet, but this finding is important for atmospheric research in the context of greenhouse gases. Such fast and highly sensitive measurements as described here would not be possible with near-infrared systems due to the lack of sensitivity and the results shown here demonstrate, that tunable diode-laser absorption spectroscopy can be a valuable tool for quality assurance and quality control.

11.3 Near-Infrared Overtone Spectrometer

For many industrial applications or field measurements the use of liquid nitrogen must be avoided, closed cycle coolers are too expensive and only thermoelectrical elements are acceptable (D´Amato and De Rosa 2002). Several molecular species have absorption features in the near infrared spectral region. Near-IR absorptions are overtone or combination bands that are typically one to several orders of magnitude weaker than the IR-fundamental band. Nevertheless, many molecules of interest have near-IR absorption bands that are strong enough for detection at parts-per-million (1 ppmv = 10^{-6} volume mixing ratio) and even parts-per-billion (ppbv) levels.

The overtone or combination band transitions can be accessed by Gallium-Arsenide and Indium-Phosphide lasers, which are commercially made from the III-V group of semiconductor materials. These diode lasers emit from the visible to near-infrared wavelengths from 0.63 µm to above 2 µm including the InGaAsP/InP lasers. The technology of the 1.3 µm and 1.55 µm InGaAsP/InP diode-lasers developed for fiber-optic telecommunication has been extended to fabricate lasers that emit up to more than 2 µm. These near- infrared multiple-quantum-well distributed-feedback (DFB) lasers have the advantages of single-mode outputs at power levels up to several milliwatts and additionally room-temperature operation.

InP-DFB-lasers developed at the Sarnoff Research Center (Princeton, NJ) with room temperature single-mode emission at $\lambda \approx 2$ µm have been used for the design of a fast carbon dioxide sensor. The DFB-laser is held inside a Peltier-cooled mount, which is fixed on a xyz-stage (Fig. 11.6a) and the laser beam is collimated by an off-axis parabola (OAP) with 10 mm diameter and 12 mm focal length. The beam is focused by a spherical mirror (f= 1m) into the center of a commercial 5 l Herriott cell. After 181 reflections, corresponding to an optical pathlength of 100 m, the beam exits the cell and is focused onto a temperature-stabilized extended InGaAs detector by another OAP. About 8% of the laser beam is coupled off by a beam-splitter and directed through a 28 cm reference cell. The optical system is prealigned with a visible diode-laser, coupled into the setup by a pellicle beam-splitter, which has to be removed during the measurements to optimize power throughput. In order to provide static as well as flux measurements at defined cell pressures, the measurement cell is equipped with a pressure sensor (MKS Baratron) and on/off-valves (at the inlet and outlet) as well as with a needle-valve at the inlet and a throttle valve at the outlet, which is part of an active pressure stabilization loop during flow measurements. The reference cell is filled with a high concentration CO_2 mixture and sealed off and is connected to the measurement cell by a temperature bridge and a differential pressure sensor. With appropriate laser power and gas concentration in the reference cell the signals from both detectors can according to Beer´s law be adjusted to have identical amplitude and shape and after system calibration using certified gas mixtures, the reference signal can be used as a secondary calibration standard.

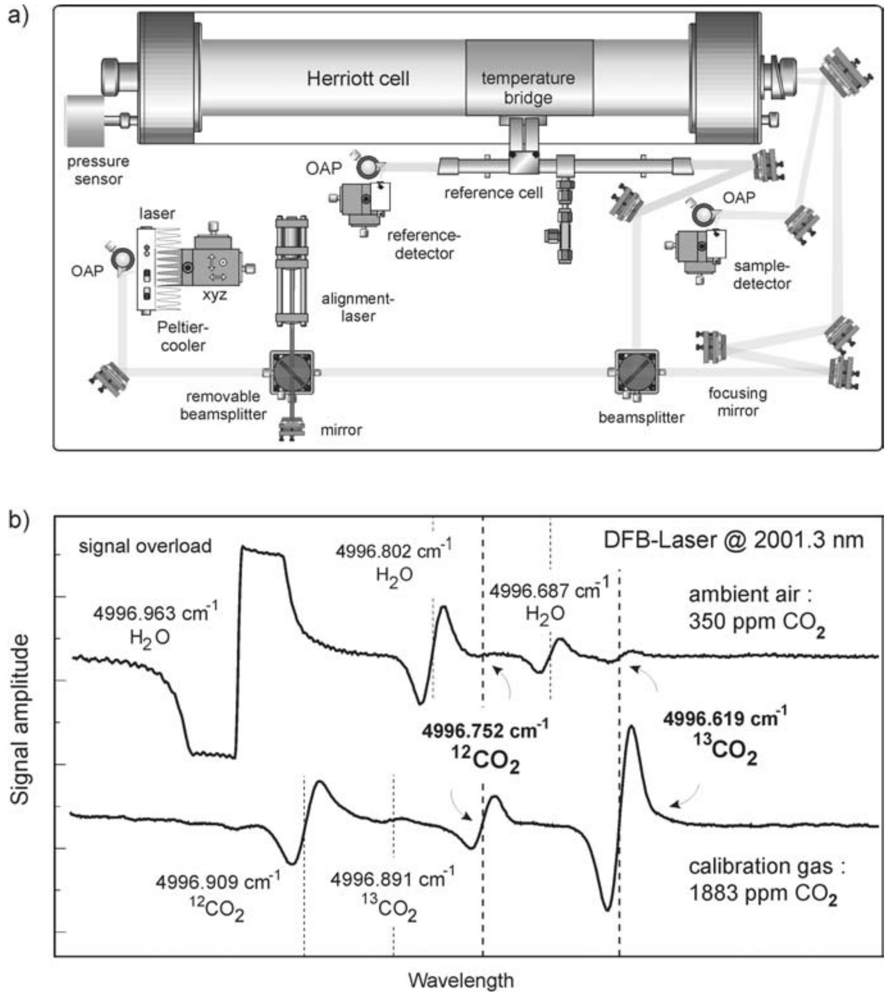

Fig. 11.6a. Optical layout of a *near-infrared* FM-spectrometer with a optical multipass cell **b.** Identification of $^{12}CO_2$ and $^{13}CO_2$ absorption near 2 µm

With this instrument a series of ambient air measurements have been performed. Time series data obtained from a 358 ppmv carbon dioxide calibration gas cylinder have been recorded and from an Allan Variance analysis, as discussed in the previous sections on the infrared measurements, a precision of about 300 ppbv has been obtained for an integration time of 1 sec. This corresponds to a minimum detectable optical density $(\alpha L)_{min}$ of 10^{-4}. The major limitation during these measurements were high transmission losses after 181 reflections in the 100 m fixed pathlength multipass Herriott cell, leading to relative low optical power levels at the detector.

The calculated detection limits in the near- and mid-infrared spectral regions are listed in Tab. 11.1 for a minimum detectable optical density of 10^{-6} for a pressure of 150 hPa and 25 m optical pathlength. The corresponding carbon dioxide spectrum is shown in Fig. 11.2.

Table 11.1 Calculated near - and mid-infrared detection limits for carbon dioxide

CO_2 Band	Wavelength λ [cm^{-1}]	 [μm]	Linestrength [cm/molec]	Detection limit [ppbv]	 [μg/m^3]
$3\,\nu_3$	6983.01	1.432	$6.043 \cdot 10^{-23}$	73	144
$2\,\nu_1 + 2\nu_2 + \nu_3$	6359.96	1.572	$1.846 \cdot 10^{-23}$	220	430
$\nu_1 + 4\,\nu_2 + \nu_3$	6240.10	1.603	$1.838 \cdot 10^{-23}$	235	461
$2\nu_1 + \nu_3$	5109.31	1.957	$4.003 \cdot 10^{-23}$	107	210
$\nu_1 + 2\nu_2 + \nu_3$	4989.97	2.004	$1.332 \cdot 10^{-21}$	3.1	6.1
$\nu_1 + \nu_3$	3597.96	2.779	$3.525 \cdot 10^{-20}$	0.11	0.22
ν_3	2361.46	4.235	$3.524 \cdot 10^{-18}$	0.002	0.004

The NIR system described above has been applied to investigate the feasibility of carbon dioxide isotopic ratio measurements and Fig. 11.6b shows an example of $^{13}CO_2$/ $^{12}CO_2$ line pairs in the 2 μm region from non-linear oscilloscope traces recorded during an investigation of line pairs (Werle et al. 1998). It is obvious from Tab. 1 that this spectral region has a significant advantage versus the 1. 57 μm absorption band in the NIR, where the line strength is about 2 orders of magnitude weaker. At 2 μm the line strength is still weaker than in the fundamental band, but room temperature operation of diode-lasers is possible for continuous wave (cw) applications (Webber 2001). Future developments of antimonide lasers might give access to the ν_1+ν_3 band near 2.78 μm, where again a significant increase in detection sensitivity can be expected. Besides atmospheric measurements, this type of instrument can be used for isotopic ratio measurements in medical diagnosis.

11.4 Quantum Cascade Lasers

Until recently all semiconductor lasers, regardless of their operating wavelength, relied upon direct band-to-band transitions in bulk material as shown in Fig. 11.7a. In such semiconductor lasers electrons recombine at the pn-junction with positively charged “holes” to release single photons with a wavelength that is determined by the bandgap, E_g , and thus the chemical composition of the semiconductor sandwich. The interband transitions between the conduction and the valence bands provide the laser radiation.

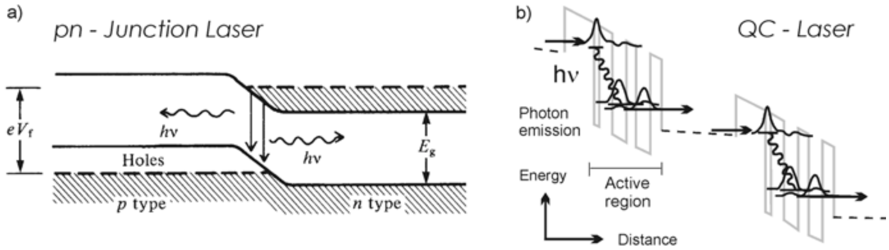

Fig. 11.7a. pn-semiconductor laser and **b.** quantum cascade laser (Faist et al. 1994)

Quantum cascade lasers are based on a completely different approach than the lasers described so far. Their operation is based on intersubband transitions, i.e. transitions within the conduction band (Fig. 11.7b) of a cascaded multiple quantum well structure. Although the basic concept was proposed as early as 1971, it took more than 20 years until an actual device was demonstrated in 1994 (Faist et al. 1994). In a pictorial way, this laser is freed from bandgap-slavery as the emission wavelength depends only on the layer thickness and not on the bandgap of the constituent materials. The quantum well structures are grown using molecular beam epitaxy as alternating layers with a thickness of a few atoms are grown of alloy materials (e.g. InGaAs and InAlAs).

The operation of the quantum cascade laser can be understood us follows. The different materials of the semiconductor in the active region have different band gaps, which leads to the creation of quantum wells. These quantum wells have discrete energy levels due to the thinness of the layers comparable to the electrons de Broglie wavelength. The electrons motion is restricted in the direction perpendicular to the plane of the layers but can move freely in the plane of the layers. An electron in the upper level of the active region will first in a slow process scatter to an intermediate sub-band producing a photon and then fast into the lowest subband. The energy levels are determined by the thickness of the layers in the active region. The stages of the QC laser consist of an area with closely spaced layers (the injection region) followed by more widely spaced layers (active region). The stack of active regions is clad with two thick semiconductor layers of low refractive index, that serve as a wave-guide to direct the produced light along the active regions. In a QCL typically 30 to 75 alternating structures of active regions and injector/relaxation regions are stacked. Once an electron is injected from the contact regions, it is forced to pass through all the periods of active regions and injectors sequentially (cascading). Once the device exceeds lasing threshold, it will emit one photon per period. Adding stages to QC lasers thus increases their output power. In lasers developed in 1999 electrons cascade down 75 steps, instead of 20 or 30 as in earlier QC lasers (i.e. producing up to 75 photons for one electron). In this way QC lasers can provide more than a thousand times the output power of any commercial semiconductor laser operating in the mid-infrared region. Such a QC laser can operate in a large number of modes at wavelengths around the one determined by the energy difference between the upper and intermediate levels. To produce stable, single-mode emission from these QC lasers, as is needed for spectroscopic applications, a grating is integrated into the laser wave-guide producing a distributed feedback device. The grating selects a single mode that satisfies the Bragg condition. Thus, continuous, single mode emission is produced with tuning ranges of about 100-150 nm (at 3-15 µm). The tuning here takes place by changing the temperature of the laser, which changes the refractive index of the wave-guide material, and thus the wavelength at which the Bragg condition holds.

Quantum Cascade-Distributed Feed Back (QC-DFB) lasers can operate either in pulsed mode up to room temperature or in cw mode, operating from cryogenic to above liquid nitrogen temperature (Köhler et al. 2000) and even room temperature cw emission of up to 17 mW at 9.1 µm has already been reported (Beck et al. 2002). In pulsed mode, heating occurs during the current pulse. This changes the emission wavelength slightly, resulting in a dynamic line-width of the laser of a few hundred MHz. Therefore, for application of high resolution spectroscopy in trace gas detection, the laser is preferably used in cw mode, in which case line-widths of a few kHz are attainable (Williams et al. 1999).

QC-DFB lasers have been reported for various wavelengths between 5.2 and 16 µm and have already been used to study gases as NO (Sharpe et al. 1998), N_20 (Namjou et al. 1998), NH_3 (Sharpe et al. 1998), CH_4 (Kosterev et al. 1999), and C_2H_4 (Hvozdara er al. 2000). A QCL-system has been flown on NASA´s ER-2 high altitude aircraft to measure stratospheric N_2O and CH_4 (Webster et al. 2001) and the number of applications is rapidly increasing (Kosterev and Tittel 2002). With the development of a QC-DFB laser operating at 4.6-4.7 µm medically important gases like CO and CO_2 and their isotopes, that have their strongest rotational-vibrational bands between 4 and 5 µm have come within range as well (Köhler et al. 2000). Quantum cascade lasers based on InGaAs/InAlAs are already commercially available and have been demonstrated in the wavelength range from 3.4 µm to 13 µm, with room temperature operation from 5 µm to 11.5 µm. Using super-lattice active regions also operation at 17 µm was demonstrated. An advantage of this super-lattice type of laser is that they can carry higher electrical currents than conventional QC lasers, which potentially provides higher output powers (0.5 W at room temperature). Using a novel design where surface plasmon modes are exploited instead of conventional dielectric wave-guides, lasers operating up to 19 µm have recently been achieved (Tredicucci et al. 2000). Other materials are also being used, e.g. GaAs/AlGaAs Systems have been demonstrated for 9.6 µm and 13 µm, and in DFB mode for 10 µm (Schrenk et al. 2000). Output of the QC lasers so far is limited on the short wavelength side of the mid-infrared spectrum by the band-offset between the quantum-well and the barrier materials. For shorter wavelengths deeper quantum wells are needed, which requires different materials. New developments are directed towards developing, lasers, which can produce shorter wavelengths by identifying and implementing new material systems, e.g. based on group III nitrides (Hofstetter et al. 2000).

11.5 Quantum Limited Spectroscopy

Diode laser spectroscopy is a valuable technique for gas analysis. The ability to provide unambiguous measurements qualifies TDLAS as a reference technique against which other methods are often compared. The technique is universally applicable to smaller infrared active molecules and the same instrument can easily be converted from one species to another by changing the laser and calibration gases. The time resolution of TDLAS measurements can be traded off against sensitivity and this allows fast measurements with millisecond time resolution. In order to improve sensitivity various types of modulation spectroscopy have been employed in which the diode laser wavelength is modulated while being scanned across an absorption line. These modulation techniques allow absorption as low as 1 part in 10^6 to be measured within a 1 Hz bandwidth. In combination with optical multipass cells this is equivalent to detection limits of around 20 pptv for the most strongly absorbing species and better than 1 ppbv for almost all species of interest.

The ultimate detection capability is, in principle, only limited by quantum noise (Ye et al. 1998). The signal-to-noise ratio (SNR) is a figure of merit for a detection system. Usually absorption spectrometers are designed in a way that the detected signal is proportional to the laser power arriving at the detector. The total noise is given by the sum of contributions from excess noise, photon induced shot noise and thermal noise, which is independent from power. If an appropriate detection scheme is selected and sufficient power is available, shot noise dominates over thermal noise. The SNR under such “quantum limited” conditions is proportional to the square root of the power impinging on the detector (Werle 1998). Such quantum limited conditions have been obtained with single optical paths (Werle et al. 1989).

In order to discuss problems that are connected with the application of multipass cells with different optical pathlength L, detection limits and other characteristic data from instruments based on White and Herriott cell designs are summarized in Table 11.2. As a figure of merit the observed minimum detectable optical density $(\alpha L)_{min}$ normalized to a $\Delta f = 1$ Hz bandwidth is included, ranging from $1 \cdot 10^{-4}$ to $5 \cdot 10^{-7}$ for different multipass setups. The highest sensitivities have been obtained with a White cell instrument, where the optical pathlength has been reduced from 100 m down to about 30 m and with a fast eddy correlation system, where the pathlength of the Herriott cell has been set to 18 m instead of the possible 36 m. In order to understand the advantage of the reduced pathlength, we have to recall that in the mid-infrared a minimum power at the detector of about 100 µW is required to make shot noise the dominating contribution and, therefore, too many reflections in the optical multipass cells deteriorate system performance significantly (Werle and Slemr 1991). With respect to the discussion of quantum limited performance, it can be seen from Table 11.2 that the best performance has been obtained for high laser power and if pathlength is reduced below maximum, as a trade-off between absorption pathlength and power throughput.

Table 11.2. Summary of characteristics and performance data of optical multipass systems

Instrument	Mid Infrared				Near Infrared
	High sensitivity		High Speed		
Target Gas	NO_2	H_2CO	CH_4	CH_4	CO_2
Wavenumber	1600 cm^{-1}	2800 cm^{-1}	3076 cm^{-1}	1290 cm^{-1}	4990 cm^{-1}
Wavelength	6.25 µm	3.57 µm	3.25 µm (ν_4)	7.8 µm (ν_3)	2.004µm
S [cm/molec]	~2x10^{-19}	~6x10^{-20}	~2x10^{-19}	~5x10^{-20}	~1x10^{-21}
Cell type	White	White	Herriott	Herriott	Herriott
Volume	6 l	6 l	5 l	0.3 l	5 l
Pressure	26.7 hPa	30 hPa	30 hPa	50 hPa	100 hPa
Path Length	27.5 m	30 m	100 m	18 m	100 m
Laser Power	1000 µW	400 µW	< 200 µW	200 µW	1700 µW
Cooling	LN_2	LN_2	LN_2	LN_2	Peltier
Detector	HgCdTe	HgCdTe	HgCdTe	HgCdTe	InGaAs
Calibration	12 ppbv	35 ppbv	1.8 ppmv	2 ppmv	358 ppmv
Type	Permeation	Permeation	Gas Cylinder	Gas Cylinder	Gas Cylinder
Precision	10 pptv	120 pptv	37 ppbv	9 ppbv	300 ppbv
Integr. Time	@ 25 sec	@ 40 sec	@ 0.06 sec	@ 0.1 sec	@ 1 sec
	(0.08%)	(0.3%)	(2%)	(0.5%)	(0.08%)
$(\alpha L)_{min}$ @ Δf=1 Hz	5 ·10^{-7}	1 ·10^{-6}	2.7 ·10^{-4}	1.5 ·10^{-5}	1 ·10^{-4}

Rapid progress has been reported in quantum cascade lasers and these lasers appear to offer the prospect of significantly higher cw-power required for quantum limited multipass systems. With a laser power of a few hundred mW a quantum limited performance is feasible together with the improvements in SNR according to the square root relationship mentioned before. Additionally, the pathlength could easily be extended and the reported detection limits would scale accordingly. For applications, where shot noise limited sensitivities are not required, an increase in signal-to-noise ratio can be used to simplify signal processing, allow less maintenance and, therefore, help to reduce operational cost. An increasing number of spectroscopic measurements with quantum cascade lasers have been reported and the commercial availability of these lasers will promote the development of new operational systems that allow new sensitive measurements based on the strong fundamental IR transitions.

TDLAS has made the transition from a technique mainly of interest to instrument developers into one which produces results of real value to industrial gas analysis and atmospheric research. The near- and mid-infrared spectral regions will provide complementary systems. For a limited number of species, where ultra-high sensitivity is not required, the near-infrared systems will provide advantages of size, simplicity and cost. For other species, requiring a more universal and sensitive system, mid-infrared lasers will continue to provide a highly specific device to meet the requirements of current and future measurement challenges.

References

Beck M, Hofstetter D, Aellen T, Faist J, Oesterle U, Ilegems M, Gini E, Melchior H (2002) Continuous wave operation of a mid-infrared semiconductor laser at room temperature. Science 295:301-305

Brassington DJ (1995) Tunable diode laser absorption spectroscopy for the measurement of atmospheric species. In : Clark RJH, Hester RE (eds) Spectroscopy in environmental science, Wiley, New York

D´Amato F, De Rosa M (2002) Tunable diode-lasers and two-tone frequency modulation spectroscopy applied to atmospheric gas analysis. Optics & Lasers in Eng 37:533-551

Fischer H, Wienhold FG, Hoor P, Bujok O, Schiller C, Siegmund P, Ambaum M, Scheeren HA, Lelieveld J (2000) Tracer correlations in the northern high latitude lowermost stratosphere : Influence of cross-tropopause mass exchange. Geophys Res Lett 27:97-100

Fried A, Sewell S, Henry B, Wert B, Gilpin T, Drummond JR (1997) Tunable diode laser absorption spectrometer for ground-based measurements of formaldehyde. J Geophys Res 102:6253-6266

Faist J, Capasso F, Sivco DL, Sirtori C, Hutchinson AL, Cho AY (1994) Quantum cascade laser. Science 264:553-555

Herriott DR, Schulte HJ (1965) Folded optical delay lines. Appl Opt 4:883-889

Hofstetter D, Faist J, Bour DP (2000) Mid-infrared emission from InGaN/GaN-based light emitting diodes. Appl Phys Lett 76:1495-1497

Hvozdara L, Gianordoli S, Strasser G, Schrenk W, Unterrainer K, Gornik E, Murthy Ch, Kraft M, Pustogov V, Mizaikoff B (2000) GaAs/AlGaAs quantum cascade laser – a source for gas absorption spectroscopy. Physica E 7:37-39

Köhler R, Gmachl K, Tredicucci A,Capasso F, Sivco DL, Chu SNG, Cho AY (2000) Single mode tunable, pulsed and continuous wave quantum cascade distributed feedback lasers at $\lambda \cong 4.6$-4.7 µm. Appl Phys Lett 76:1092-1094

Kormann R, Müller H, Werle P (2001) Eddy flux measurements of methane over the fen Murnauer Moos, 11°11´E, 47°39´N, using a fast tunable diode laser spectrometer. Atmos Env 35:2533-2544

Kosterev AA, Curl RF, Tittel FK, Gmachl C, Capasso F, Sivco DL, Baillargeon JN, Hutchinson AL, Cho AY (1999) Methane concentration and isotopic composition measurement with a mid-infrared quantum-cascade laser. Opt Lett 24:1762-1764

Kosterev AA, Tittel FK (2002) Chemical sensors based on quantum cascade lasers, IEEE J of Quant Elect 38:582-591

Namjou K, Cai S, Whittaker EA, Faist J, Gmachl C, Capasso F, Sivco DL, Cho AY (1998) Sensitive absorption spectroscopy with a room-temperature distributed-feedback quantum-cascade laser. Opt Lett 23:219-221

Nicolas JC, Baranov AN, Cuminal Y, Roillard Y, Alibert JC (1998) Tunable diode laser absorptions spectroscopy of carbon monoxide around 2.35µm, Appl Opt 37:7906-7911

Rothman LS, Gamache RR, Tipping RH, Rinsland CP, Smith MAH, Brenner DC, Malathy Devi V, Flaud JM, Camy-Peyret C, Perrin A, Goldman A, Massie ST, Brown LR, Toth RA (1992) Hitran molecular database. J Quant Spectrosc Radiat Transfer 48:469-507

Schiff HI, Mackay GI, Bechara J (1994) The use of tunable diode laser absorption spectroscopy for atmospheric measurements. In : Sigrist MW (ed) Air monitoring by spectroscopic techniques, Wiley, New York

Schrenk W, Finger N, Gianordoli S, Hvozdara L, Strasser G, Gornik E (2000) GaAs / AlGaAs distributed feedback quantum cascade lasers, Appl Phys Lett 76:253-255

Sharpe SW, Kelly JF, Hartman JS, Gmachl C, Capasso F, Sivco DL, Baillargeon JN, Cho AY (1998) High-resolution (Doppler-limited) spectroscopy using quantum cascade distributed-feedback lasers. Opt Lett 23:1397-1398

Tacke M (1995) New developments and applications of tunable IR lead-salt lasers. Infrared Physics and Technology 36:447-463

Tredicucci A, Gmachl C, Wanke MC, Capasso F, Hutchinson AL, Sivco DL, Chu SNG, Cho AY (2000) Surface plasmon quantum cascade lasers at $\lambda \cong 19$ µm. Appl Phys Lett 77:2286-2288

VDI Kompetenzfeld Optische Technologien (2002) Applications and trends in optical analysis technology - VDI Berichte 1667. VDI Verlag, Düsseldorf

Webber ME, Claps R, Englich FV, Tittel FK, Jeffries JB, Hanson RK (2001) Measurements of NH_3 and CO_2 with DFB diode lasers near 2.0 µm in Bioreactor vent gases. App Opt 40:4395-4403

Webster CR, Flesh GJ, Scott DC, Swanson JE, May RD, Woodward WS, Gmachl C, Capasso F, Sivco DL, Baillargeon JN, Hutchinson AL, Cho AY (2001) Quantum cascade laser measurements of stratospheric methane and nitrous oxide. Appl Opt 40:321-326

Werle P (1998) A review of recent advances in semiconductor laser based gas monitors. Spectrochimica Acta A54:197-236 with 197 references

Werle P, Slemr F (1991) Signal-to-noise ratio analysis in laser absorption spectrometers using optical multipass cells. Appl Opt 30:430-434

Werle P, Lechner S (1999) Stark-modulation-enhanced FM-Spectroscopy. Spectrochimica Acta A55:1941-1955

Werle P, Popov A (1999) Application of Antimonide lasers for gas sensing in the 3-4 µm range. Appl Opt 38:1494-1501

Werle P, Kormann R (2001) Fast chemical sensor for eddy correlation measurements of methane emissions from rice paddy fields. Appl Opt 40:846-858

Werle P, Mücke R, Slemr F (1993) Limits of signal averaging in atmospheric trace gas monitoring by tunable diode laser absorption spectroscopy. Appl Phys B57:131-139

Werle P, Scheumann B, Schandl J (1994) Real time signal-processing concepts for trace-gas analysis by diode-laser spectroscopy. Opt Eng 33:3093-3105

Werle P, Slemr F, Gehrtz M, Bräuchle Chr (1989) Quantum-limited FM-spectroscopy with a lead-salt diode-laser. Appl Phys B49:99-108

Werle P, Mücke R, D´Amato F, Lancia T (1998) Near-infrared trace-gas sensors based on room-temperature diode lasers. Appl Phys B67:307-315

Werle P, Slemr F, Maurer K, Kormann R, Mücke R, Jänker B (2002) Near- and mid-infrared laser-optical sensors for gas analysis. Optics & Lasers in Eng 37:101-114

White JU (1976) Very long optical paths in air. J. Opt.Soc. Am. 66:411-416

Williams RM, Kelly JF, Hartmann JS, Sharpe SW, Taubmann MS, Hall JL, Capasso F, Gmachl C, Sivco DL, Baillargeon JN, Hutchinson AL, Cho AY (1999) Kilohertz linewidth from frequency stabilized mid-infrared quantum cascade lasers. Opt Lett 24:1844-1846

Ye J, Ma LS, Hall JL (1997) Ultrasensitive detections in atomic and molecular physics : demonstration in molecular overtone spectroscopy. J Opt Soc Am B 15:6-14

Zahniser MS, Nelson DD, McManus JB, Kebabian PL (1995) Measurement of trace gas fluxes using tunable diode laser spectroscopy. Phil. Trans. R. Soc. Lond. 351:371-382

Springer

http://www.springer.com/978-3-540-40260-2

Laser in Environmental and Life Sciences
Modern Analytical Methods
Hering, P.; Lay, J.P.; Stry, S. (Eds.)
2004, XXIV, 347 p., Hardcover
ISBN: 978-3-540-40260-2